chapter **SEVEN**

ONE-STEP SURGICAL PROCEDURE FOR THE TREATMENT OF OSTEOCHONDRAL DEFECTS WITH ADIPOSE-DERIVED STEM CELLS IN A CAPRINE KNEE DEFECT: A PILOT STUDY

Wouter J.F.M. Jurgens, Robert Jan Kroeze, Behrouz Zandieh-Doulabi, Annemieke van Dijk, Greetje A.P. Renders, Theo H. Smit, Florine J. van Milligen, Marco J.P.F. Ritt, Marco N. Helder

ABSTRACT

Regenerative therapies offer attractive alternatives for the treatment of osteochondral defects. Adipose derived stromal cells (SVF) allow the development of a one-step surgical procedure by their abundant availability and high frequency. In this study we evaluated the *in vivo* osteochondral defect repair efficacies of scaffolds seeded with freshly isolated (SVF) and cultured adipose stem cells (ASC), and compared these to their acellular counterparts.

Osteochondral defects were created in medial condyles and trochlear grooves in knees of eight goats. Defects were filled by acellular collagen I/III scaffolds, or scaffolds seeded with SVF or cultured ASCs. Osteochondral regeneration was evaluated after one and four months by macroscopy, immunohistochemistry, biomechanical analysis, microCT analysis, and biochemistry.

After one month, defect appearances varied from yellow/reddish (center) to whitish/opaque (edges). Microscopic, but not macroscopic evaluation showed considerable but not significant differences, with ASC- and SVF-loaded constructs showing more extensive regeneration. After 4 months acellular constructs displayed increased regeneration, however, to a lesser degree than the cell-treated constructs. The latter exhibited more extensive collagen type II, hyaline-like cartilage, higher elastic moduli, and their glycosaminoglycan content in the cartilaginous layer better approached native tissue values. Moreover, their defect regions contained higher levels of regenerated, mature subchondral bone with more intense collagen type I staining. SVF performed best on all parameters.

Summarizing, this pilot study demonstrated the preclinical feasibility of a one-step surgical procedure for osteochondral defect regeneration, with most optimal results using freshly isolated adipose stromal cells, Larger studies with longer follow-up are required to substantiate these findings**.**

INTRODUCTION

Tissue engineering therapies are being evaluated as promising alternatives to heal (osteo)chondral defects. These defects have limited self regenerative potential or result in suboptimal functional repair when using conventional joint resurfacing treatments[1-4]. Adipose tissue is an attractive source of stem cells for these regenerative therapies due to its abundance, high frequency of stem cells, and their multilineage differentiation capacity[5]. Currently, most therapies focus on the use of cultured cells of various origin to obtain sufficient quantities needed for regeneration[3,6-10]. The use of adipose tissue can overcome this culturing step since a clinically relevant number of stem cells can be isolated, creating the possibility to develop a one-step surgical procedure (OSP) for the treatment of osteochondral defects[11]. This concept was already tested *in vitro* before and showed promising results, demonstrating the ability of the ASC fraction within the stromal vascular fraction (SVF) to attach to a scaffold material in sufficient quantities in a short time frame (~10 min), and the capacity to differentiate into the osteogenic and chondrogenic lineage.[12,13]. Obvious advantages of this approach in humans can be found in its patient-friendliness and its lower costs, since a second surgical intervention and expensive *in vitro* culturing steps would be avoided.

To further investigate the feasibility of this one-step surgical procedure for the treatment of osteochondral defects, we employed an *in vivo* goat model. To evaluate the potential modulatory effects of other cell types present in the SVF, scaffolds seeded with freshly isolated adipose derived stromal cells were compared with scaffolds seeded with adipose derived stem cells cultured to homogeneity. Bare, acellular scaffolds were introduced as negative control.

MATERIALS AND METHODS

Experimental animals

Eight skeletally mature female Dutch milk goats (at least 3.5y old) with an average body weight of 82.4 ± 11.7 kg were used in this study. Protocols were approved by both a Scientific Board as well as the Animal Ethics Committee of the VU University Medical Center.

Surgical procedures

Animals were considered healthy based on physical examination, and viral and bacterial tests. Anaesthesia was induced with a combination of 10 mg/kg of body weight ketamine (Alfasan, Woerden, The Netherlands), 1.5 mg Atropine (Pharmachemie, Haarlem, The Netherlands) and 10-20 mg Etomidate I.V. (B.Braun, Melsungen, Germany). After endotracheal intubation goats received a bolus of 15 mg Midazolam I.V. (Dormicum, Actavis B.V. Baarn, The Netherlands) which was repeated if indicated. Anaesthesia was maintained with 1- 2 % Isoflurane per inhalation. Perioperative analgesia was achieved by administering 250 μL Fentanyl I.V. (Hameln Pharmaceuticals, Hameln, Germany), and penicillin and streptomycin were administered as perioperative antibiotics. Postoperative

analgesia consisted of one administration of Buprenorfine I.M. (Temgesic, Schering-Plough B.V.,Utrecht, The Netherlands), and maintained for 7 days with Novum 20 S.C. (Meloxicam, Boehringer Ingelheim B.V. Alkmaar, The Netherlands).

All goats underwent surgery twice: during the first procedure adipose tissue was harvested for culturing of cells. An incision was made along the left thoracolumbar vertebrae, underlying subcutaneous adipose tissue was dissected (± 30 g) and processed for SVF (see below), which was subsequently cultured to obtain a homogenous population of ASC. After surgery goats were allowed to move freely. Two weeks later, adipose tissue was harvested again but now from the right thoracolumbar region, to procure freshly isolated SVF. This second harvesting/processing step was followed by implantation surgery (see below).

Adipose derived stem cell procurement and culturing

SVF was isolated from each goat as described previously[14]. In short, adipose tissue was dissociated with 0.5 U/mL Liberase Blendzyme 3 (Roche Diagnostics, Almere, The Netherlands), and subsequently passed through a 100 µm-mesh filter (Stokvis & Smith B.V., IJmuiden, The Netherlands) to remove debris. The resulting single-cell suspension was pelleted and washed several times with PBS. The resultant stromal vascular fraction (SVF) was either implanted directly in the one-step surgical procedure (surgery 2), or used for culturing to obtain a homogeneous population of ASC (surgery 1). A small fraction of each SVF was used for colony-forming unit assays to determine the percentage of stem cells within the preparations (see below). For culturing, SVF was plated in 25 cm^2 tissue culture flasks. Medium consisted of Dulbecco's modified Eagle's medium (DMEM, Gibco, Paisley, UK) supplemented with 10% fetal bovine serum (FBS; Hyclone, Logan, UT, USA), 100 U/mL penicillin, 100 µg/mL streptomycine and 2 mM L-glutamine (all Invitrogen, Gibco). Cultures were grown in a humidified incubator at 37°C in an atmosphere of 5% CO_2. When reaching 80-90% confluency, cells were detached with 0.5 mM EDTA/0.05% trypsin (Invitrogen) for 5 min at 37°C, and replated. In this way a homogeneous population of ASCs was obtained. Cultured ASCs were used for implantation at passage 3 in surgery 2.

Colony-forming unit-fibroblast assays (CFU-f assay)

CFU-f assays were performed as described previously[15]. In short, two 6-well plates were prepared with 10^4 nucleated SVF cells in the upper and 10^3 cells in the lower row respectively. Colony formation was allowed for 7-10 days, depending on number and growth kinetics of the colonies (merging of colonies was avoided). After fixation, colonies were stained with 0.2% toluidine blue solution in borax buffer, and counted.

Implant preparation

Treatment groups existed of phosphate buffered saline (PBS), freshly isolated SVF ($5*10^6$ cells) and cultured ASCs ($5*10^5$ cells). The three different mixtures were seeded in 70 µL onto a Ø 5x3mm high collagen type I/III scaffold (Optimaix®, Matricel GmbH, Herzogenrath, Germany) which *in vitro* was shown to allow chondrogenic differentiation[13] and after 30 min implanted into the defect.

Implantation surgery

Animals were prepared for surgery as described above. Two preceding pilot experiments showed that i) suturing to adjacent healthy cartilage was not sufficient to ensure scaffold retainment; ii) poly lactide-co-glycolide membrane coverings got detached; and iii) commercial fibrin glue (Tissucol, Baxter, Vienna, Austria) caused a massive giant cell reaction (Suppl 1). Therefore, it was decided to make a medial parapatellar incision to expose the right knee joint, and to create two reproducible fresh critically sized osteochondral defects (Ø 5 mm, depth 3.5 mm)[16,17] in the right trochlea femoris and the right medial femoral condyle (4 in total per animal). This was achieved using a custom-made grinder and holder. As a result, each goat was treated with one or two (randomised per each two goats) SVF and ASC-loaded scaffolds, and one acellular control. Accordingly, in total 12 SVF- and ASC-treated constructs and 8 acellular scaffolds were implanted. Scaffolds recessed just under the articular surface to minimize early shear stress. A small drop of synovial fluid was added to induce swelling and press-fitting of the implant in the defect site. For additional retainment, prolene® 5-0 cross-suturing was applied (attached to the cartilage ± 3 mm from the defect border to minimize possible adverse effects). The wounds were closed in layers using Vicryl® 2-0 sutures.

A full-limb cast (Softcast®, 3M, Zoeterwoude, The Netherlands) was applied for 1 month, which restricted the range of motion to about 5°[18], caused only minor restriction of the gait, but did not affect the weight bearing fuction of the limb. After 1 month, two goats (containing three SVF and ASC-loaded scaffolds, and two acellular scaffolds), were sacrificed using a lethal dose of pentobarbitalnatrium (Euthasol 20%, Ast Beheer B.V., Oudewater, The Netherlands), whereas the casts of the remaining 6 goats were removed and free movement for the ensuing 12 weeks was allowed before sacrifice.

Sample preparation and assessment

Upon sacrifice, gross resemblance of the newly formed tissue in the defects was scored using the method of Moran et al.[19]. The 1-month samples were processed for histology only, whereas the 4-month samples were first analysed mechanically (see below), followed by splitting the specimens into two equal parts. One part (+surrounding tissue) was used for microCT analysis followed by histology whereas the other part (scaffold area only) was processed for biochemistry (SVF: n=9, ASC: n=8, PBS: n=7). Undamaged control cartilage pieces from the same implantation site were collected to serve as positive controls.

Mechanical analysis

Each specimen assigned for mechanical analysis was tested with a specially designed benchtop indenter (Suppl 2). Specimens were immersed in PBS to prevent fluid loss. The measurement set-off point was determined by putting the indenter at the surface of each specimen until the stress force increased with 10 μN. The tensile stress-relaxation property of each specimen and its native cartilage control was determined at increasing steps of 50, 100, 200, and 300 μm indentation at a constant speed of 20 μm/s with a 4 mm diameter bold-tip probe. These indentation depths were chosen based on previous studies[6,20,21] and proven reliable for determination of response force and calculation of elastic modulus in a pilot experiment (data not shown). The response force was recorded as a function of time

using a stress gauge on the base of the specimen and transformed to compressive stress by Labview Software®. Next, the elastic or Young's modulus could be calculated using Hertz equation[22], setting *v* at 0.30[23], using the following equation:

$$(1)\ F = \frac{2^{3/2} * 4R^{1/2}}{3\left(\left(1 - v^2\right)/E\right)}$$

To correct for variation of implantation site, results were also depicted as percentage of each sample compared to the adjacent native cartilage tissue.

Semi-quantitative histological analysis

The histological specimens were fixed in 10% formalin, decalcified, embedded in paraffin, and cut into 6 µm-thick sagittal sections. Sections were stained using standard hematoxylin/eosin, and adjacent sections with Alcian blue for the detection of proteoglycans. Digital images were obtained using a Leica microscope and Leica QWin V3 software. Semi-quantitative histological scoring was performed according to the modified cartilage repair scoring system used by other authors[19,24-27], which has been evaluated as a reliable and reproducible scoring system[28]. The following parameters were assessed: tissue hyalinity (absence of coarse collagen fibers), metachromatic staining of the matrix with Alcian blue, surface irregularity, chondrocyte clustering, regenerated subchondral bone, bonding to the adjacent articular cartilage, inflammatory cell infiltration around the implant, and freedom from degenerative changes in the adjacent cartilage, with a maximum score of 21 (best result). Assessments were performed by two independent observers, which were blinded to reduce observational bias. The representative score for each parameter was determined by averaging scores of the two independent observers and reported separately under each independent parameter to be able to compare each parameter for the three different groups with the other.

Immunohistochemical staining

Expression of collagen type I and II was studied by immunohistochemical staining against collagen type I (ab23446, Abcam, Cambridge, UK) and collagen type II (II-II6B3, Developmental Studies Hybridoma Bank, Iowa, USA). Immunohistochemical staining against collagen type II was performed as previously described[15]. Briefly, sections were pretreated with pronase and hyaluronidase, incubated with a 1:50 dilution of the primary antibody at 4ºC overnight, and presence of type II collagen was visualized by Dako REAL™ EnVision™/HRP (Dako, Carpinteria, CA) with 3,3'-Diaminobenzidine (DAB) solution as substrate.

For staining of collagen type I, sections were pretreated with 10 µg/mL proteinase K for 30 min, incubated with 1:100 dilution of monoclonal mouse collagen type I at 4ºC overnight, and visualized by Dako REAL™ EnVision™/HRP (Dako) in combination with DAB solution.

Contrast-enhanced microCT analysis

A µCT-40 system (Scanco Medical AG, Brüttisellen, Switzerland) was used to obtain and assess 3D reconstructions of both bone and articular cartilage. Per scan, eight samples were placed in a cylindrical specimen holder (diameter 35 mm) and scanned in air with

a resolution of 18 μm at 55 kV, 177 μA and 750 ms integration time. A reservoir on the bottom of the specimen holder contained a standardized volume of 4 mL PBS to prevent dehydration. All samples were scanned before and after a cartilage contrast-enhancement procedure. The latter procedure comprised immersion in 150 mL 40% Hexabrix 320 contrast agent (Guerbet Nederland BV, The Netherlands) for one hour at 37°C, after which samples were gently patted dry and immediately transferred to the microCT system for scanning[29]. The contrast enhancement technique exploits the negative charge of sulfated glycosaminoglycans (sGAGs) within the ECM by assuming an inverse relationship between Hexabrix accumulation and sGAGs. Hence, high X-ray attenuation readings (corresponding to high concentrations of Hexabrix) would therefore indicate regions of sGAG depletion[30,31].

Several volumes of interest (VOIs) were selected in the bone and overlying articular cartilage regions of each biopsy. For the bone reconstructions, the VOI matched the original cylindrical defect dimensions (divided in half, Fig 4j) and the adjacent native bone. For the articular cartilage reconstructions, the VOI contained the overlying soft tissue of the experimental defects and directly neighbouring cartilage, or the "healthy" cartilage samples taken from a larger distance. Next, bone or cartilage 3D reconstructions were obtained using different thresholds that allowed segmentation of both tissues. Attenuation values within the bone reconstructions were considered proportional to the local degree of mineralization of bone (DMB), being equivalent to the concentration of hydroxyapatite (HA)[32], and quantified by comparing the attenuation coefficients with reference measures of a phantom containing 0, 200, 400, 600, and 800 mg HA/cm^3. Within the cartilage, reconstructions the attenuation values were considered proportional to the distribution and average number of sGAGs.

The average bone volume fraction (BV/TV), degree of mineralized bone (DMB), and cartilage attenuation value were calculated using Scanco software.

Extracellular Matrix Biosynthesis

Quantification of the deposit of extracellular sGAGs was only assessed in the 4 month-samples. The original implant area was digested in 3% papain solution buffer overnight at 60°C. sGAGs were measured using a Blyscan kit according to the manufacturer's protocol (Biocolor LTD, Carrickfergus, Nothern Ireland). Both samples and native tissue were measured in three different concentrations in duplo to ensure measurement in the linear range. Results were depicted as the total glycosaminoglycan production per gram of tissue, as well as percentage of native tissue to overcome variation in glycosaminoglycans due to difference in implantation site.

Statistics

Kolmogorov-Smirnov tests were used to determine normalcity of measurements and, if appropriate, their logarithmics. For evaluation of semi-quantitative histological scores the Friedman ranked test was performed. Biochemical, mechanical analysis and microCT scores were evaluated using a univariate ANOVA to determine significant differences between the three groups, taking the implantation site into account as covariate, and

also treatment over native tissue analysis was performed to exclude any covariates. All statistical tests used a significance level of α=0.05.

RESULTS

Macroscopy

All goats tolerated the surgery well, and no side effects occurred during and after surgery. Goats partly immobilized in Softcast® gradually increased mobilization in the postoperative period. Upon cast removal after 1 month, goats quickly returned to normal gait.

No signs of osteoarthrosis were observed in any of the knees after 1 month (Suppl 3), despite the substantial knee joint area covered by the defects. At this time point, all groups had the same gross appearance score (Table I, maximum 8 points (range of motion excluded due to immobilization)), even though defect edges varied from yellow/reddish to whitish/opaque. Defects were still transparent with minimal repair tissue filling the defect in all groups (Fig 1a,b).

Gross appearance scores after 4 months increased significantly when compared with 1 month (Maximum 12 points, Table I) but not significantly among the three groups. However, in general surfaces appeared more whitish/opaque at the trochlear groove than at the medial condyle, thus more resembling the native tissue (Fig 1c,d). All SVF- and ASC-treated groups showed good integration with the native cartilage at the defect margins, with defect borders being barely visible. Predominantly at the medial condyle, slightly reduced cartilage thickness was still present in the center of the defect, likely because implant height was calculated to be somewhat below the cartilage surface. Moreover, a few defects in the ASC-treated group (n=3) showed marks of inflammation and concomitant osteoarthritic degeneration (mainly cartilage erosion) (Suppl 3). Defects in the acellular group also showed signs of regeneration, although surfaces appeared more yellow/reddish than in the cell-treated defects with only a thin cartilaginous coverage which did not reach up to the cartilage surface (Fig 1d).

Histological evaluation and semi-quantitative scoring

After 1 month no scaffold loss had occurred. Some differences were clearly distinguishable between the different treatment groups. Overall trend in regeneration score: ASC-treated

Table I. *Macroscopic and microscopic score of implanted constructs*

Macroscopy	SVF (n)	ASC (n)	Acellular (n)
1 month	2.7 ± 0.6 (3)	2.3 ± 0.6 (3)	2.5 ± 0.8 (2)
4 months	7.9 ± 1.2 (8)	6.1 ± 2.0 (9)	6.9 ± 2.0 (7)
p-value	<0.00001	<0.001	<0.01
Microscopy			
1 month	6.2 ± 1.3 (3)	10 ± 4.7 (3)	6.3 ± 0.4 (2)
4 months	15.0 ± 2.7 (8)	11.9 ± 3.1 (9)	13.4 ± 3.2 (7)
p-value	<0.01	<0.05	<0.01

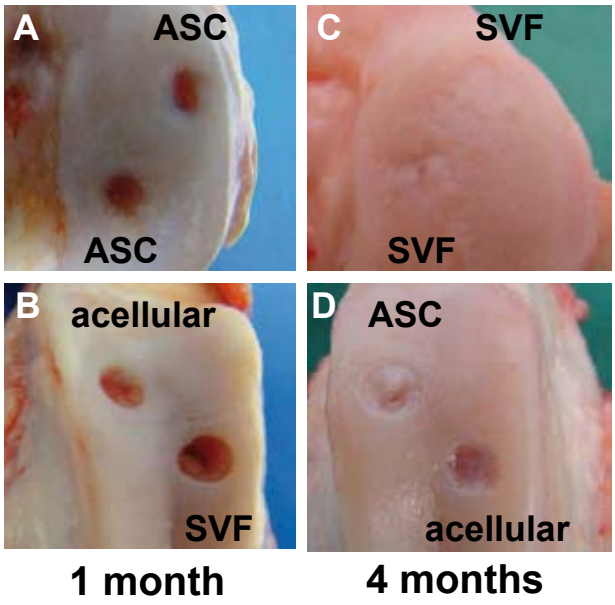

Figure 1. *Gross appearance of implantation site after 1 month (A,B) and 4 months (C,D) of implantation, showing variable cartilage regeneration. (A,B) Defects are still transparent with minimal repair tissue in all groups (C,D) After 4 months the SVF-treated group clearly shows regenerated cartilaginous tissue, with a smooth surface and hardly visible defect border (C). The ASC-treated group shows regeneration of the cartilage, with a smooth surface and good cartilage integration; however a minor defect remains in the centre (D). The acellular group shows some regeneration, with a depressed surface and only a thin cartilaginous coverage (D).*

group > the acellular group > the SVF-group (Table I). However, due to low defect numbers (SVF, n=3; ASC, n=3; acellular, n=2), this difference did not reach significance (p=0.37). More specifically, when comparing the cultured ASC with freshly isolated SVF and acellular scaffolds, the surface of the ASC-filled defect sites was more regular with less depression, less inflammatory cells, and less chondrocyte clustering (Fig 2a-c). Strikingly, 2 out of 3 ASC-treated defects were already healed with cartilaginous tissue as visualized with Col 2 (B) and Alcian Blue (C) staining and with some restoration of the subchondral bone. Remarkably, in all groups, remnants of the suture material were visible *in* the scaffold material.

After 4 months of implantation, semi-quantitative scores for all groups increased significantly compared to the 1 month counterparts (Table I). In the ASC-treated group (Fig 3a-d) 5 out of 9 defects healed, whereas 3 out of 9 defects suffered from chronic inflammation, hampering subchondral bone regeneration. In the healed defects, the newly formed cartilage had a smooth and equally high surface as the surrounding native cartilage, and showed full integration with the latter. One construct showed overall hyaline-like cartilage morphology with flat cells in the superficial and a partially columnar arrangement in the deeper zones, whereas 6 out of 9 defects were only partially filled with

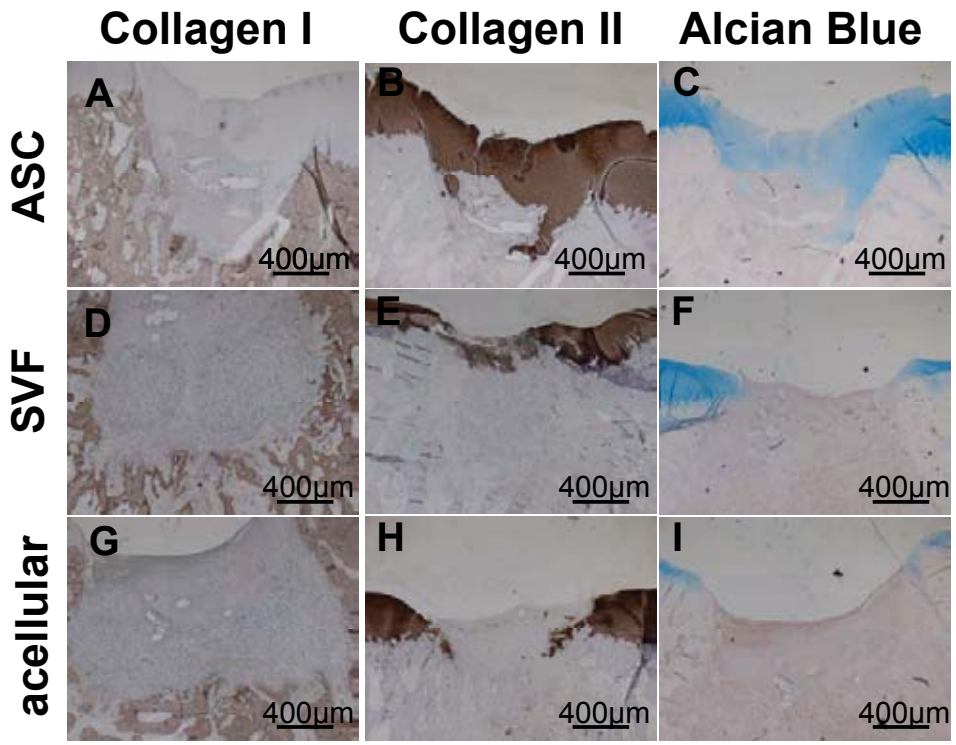

Figure 2. *Representative histological and immunohistochemical staining of ASC-treated (A-C), SVF-treated (D-F) and acellular group (G-I) after 1 month of implantation. (A-C) Some regeneration of the cartilage could be visualised in the ASC-treated group, with little depression, some restoration of the subchondral bone (A), and clear Col 2 (B) and Alcian Blue (C) staining. (D-F) little cartilage regeneration was present in the SVF-treated group, as seen by depression of the cartilage, no regeneration of the subchondral bone (D), and faint Col 2 (E) and Alcian Blue (F) staining. (H-J) There was no regeneration of cartilage and subchondral bone in the acellular group. Bars represent 400 µm.*

hyaline-like cartilage. One defect was filled with fibrous tissue only. Defects treated with the SVF-seeded construct regenerated somewhat better (Fig 3e-h), with smooth surface continuous with the surrounding cartilage in 6 out of 8 defects, and integration with adjacent healthy cartilage in all defects. Three out of 8 regenerated defects displayed full-thickness, and the remaining 5 partial hyaline-like morphology. There were no signs of inflammation. The acellular defects (n=7) regenerated to a variable extent (Fig 3i-l), with 4 defects reaching the surface level of the surrounding cartilage, of which 3 were covered with hypertrophic fibrous tissue. Partial hyaline-like cartilage was present in 5 out of 7 defects, whereas the remaining two consisted of fibrous tissue only.

Overall, more distinct bone regeneration was visible in the medial condyle vs. trochlear groove in all groups. In the ASC-treated group, subchondral bone was restored more than half with trabecular bone, in contrast with the 3 inflamed defects which showed signs of

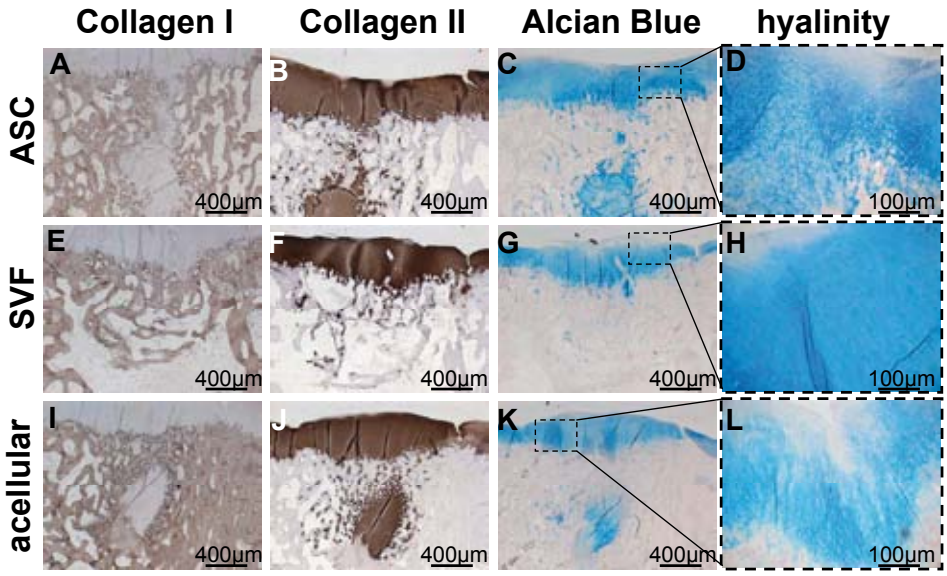

Figure 3. *Representative histological and immunohistochemical staining of ASC-treated (A-D), SVF-treated (E-H) and acellular group (I-L) after 4 months of implantation. (A-D) Clear regeneration of the cartilage could be visualised in the ASC-treated group, with little depression, almost complete restoration of the subchondral bone (A), and abundant Col 2 (B) and metachromatic Alcian Blue (C) staining, but fibrocartilaginous architecture (D). (E-H) Extensive cartilage regeneration was present in the SVF-treated group, as seen by little depression of the cartilage, almost complete regeneration of the subchondral bone (E), abundant Col 2 (F) and metachromatic Alcian Blue (G) staining, and a hyaline-like architecture of the cartilage (H). (I-L) Regeneration of cartilage and subchondral bone in the acellular group varied, with variable depression and subchondral bone regeneration, variable cartilage regeneration, metachromatic matrix staining and a fibrocartilagenous architecture (M). Bars represent 400 µm.*

bone necrosis and cyst formation (data not shown). Subchondral bone regeneration was most advanced in the SVF-treated defects, whereas acellular constructs performed least: partial subchondral bone regeneration was observed in five, and no bone filling at all in 2 out of 7.

Due to high variability, the overall histological score between all groups did not reach significance (p=0.07). If ranked and individually scored for all items, a significant difference was detected between the SVF-treated and ASC-treated group (p=0.02). A trend could be found between the SVF and untreated group (p=0.07), whereas no significance was detected between the ASC-treated and untreated group (Suppl 4).

MicroCT analysis

Implants were analysed after 4 months for bone and cartilage structure separately, the latter after contrast enhancement using Hexabrix. Remind that the relation between attenuation and proteoglycans is inversely related, so the more proteoglycans, the less

attenuation (and Hexabrix uptake by the tissue). ASC- and SVF-treated groups best resembled native proteoglycan deposition (cf. defect area and adjacent cartilage in Fig 4a-c). However, both groups did not show significant differences in attenuation (p=0.85), as can be deduced from Fig 4h. When expressed as percentage of the native tissue, differences dropped to p=0.47, with cell-treated groups best approaching the native tissue; the SVF-treated group tended to perform even better than the ASC-treated group.

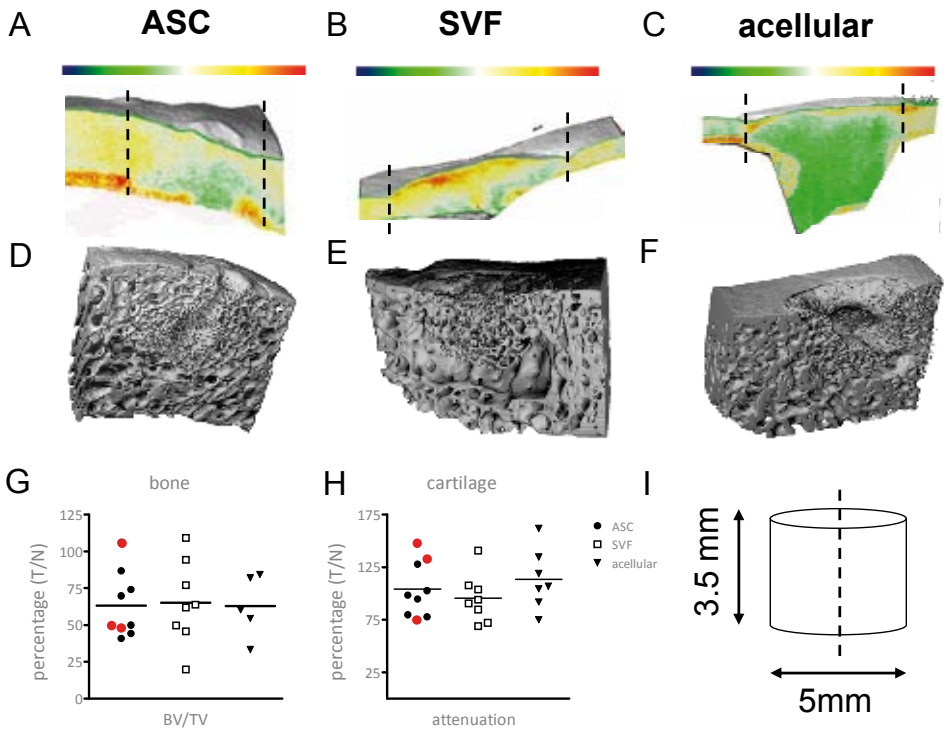

Figure 4. *MicroCT analysis of representative cartilage (A-C) and bone (D-F) explants of the ASC-treated (A,D), SVF-treated (B, E) and acellular (C, F) groups. Colours in explants A-C represent cartilage attenuation (the greener, the more proteoglycans). The cartilage in the ASC- and SVF-treated group (between dotted lines indicating defect borders) resembled the adjacent native cartilage more, indicative of better regeneration. (D-F) ASC- and SVF-treated groups showed more bone regeneration compared to the acellular group, though not significant. (G-H) Bone and cartilage characteristics of the acellular, SVF- and ASC treated groups. Results are depicted as treatment over native values (T/C). All characteristics were in slight favour of the SVF-treated group, however due to considerable variation in both bone volume to total volume (BV/TV) and cartilage attenuation, no significance was reached. Samples encircled in red suffered from chronic inflammation. In the acellular group two values are missing due to technical flaws (G). (I) Dimensions of the original defect; the dotted line represents the sagittal cutting plane, through which explants were cut in half. One of the resultant semi-circular defects was used for microCT analysis.*

ASC- and SVF-treated groups showed more bone regeneration when compared with the acellular group (Fig 4d-f). A small difference could be detected in the bone volume/total volume (BV/TV) in favour of the SVF-treated group when compared with the ASC-treated group, although not significant (p=0.28) (Fig 4g). The bone maturity, deduced from the number of trabeculae per bone volume, decreased from SVF-seeded to ASC-seeded to acellular constructs (data not shown). The degree of mineralized bone (DMB) of the regenerated bone was similar in all three groups, being approximately 92% of the native tissue (Suppl 5).

Extracellular Matrix Biosynthesis

After explantation all samples of the 4 months period were analyzed for sGAG synthesis. Determination of sGAG synthesis in the 4-months explants showed it to be independent of the implantation site (data not shown). Statistical analysis verified that due to the large heterogeneity in sGAG synthesis values in the SVF- and ASC-loaded constructs, in both cellular groups one outlier had to be excluded. The sGAG formation decreased from the SVF-treated group to the ASC-treated group to the acellular group, although no significant differences between groups could be detected (p=0.65, Fig 5). Remarkably, when averaging the individual values within each group, all groups had about similar sGAG contents as the native tissue.

Mechanical analysis

Four months' samples were explanted and the functionality of the regenerated cartilage was evaluated by submitting them to a customised indentation test (SVF: n=9, ASC: n=8, acellular: n=7). Compressive stress-relaxation represented time-dependent mechanical response to the applied load.

A significant difference could be detected between the elastic modulus of the native cartilage of the medial condyle (1.23 ± 0.57) and trochlear groove (0.45 ± 0.14, p<0.05). However, no significance was reached when comparing the three treated groups, taking into account variation due to difference in implantation site (p=0.32, Fig 6a). To exclude

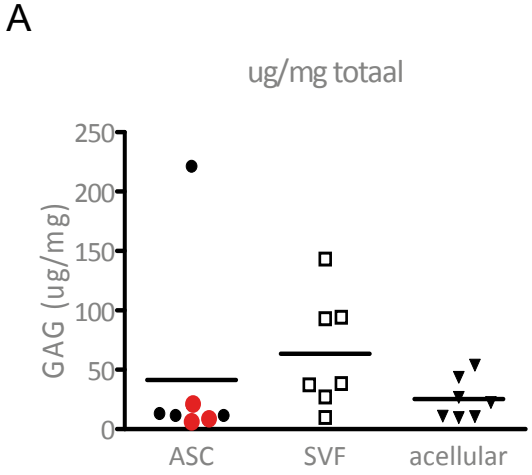

Figure 5. *GAG formation of constructs after 4 months of implantation. (A) GAG synthesis corrected for the weight of tissue. The SVF-treated group showed the highest GAG formation, followed by the ASC-treated group and finally the acellular group. Based on statistical considerations 3 samples were excluded as outliers (one in SVF-treated group, two in ASC-treated group).*

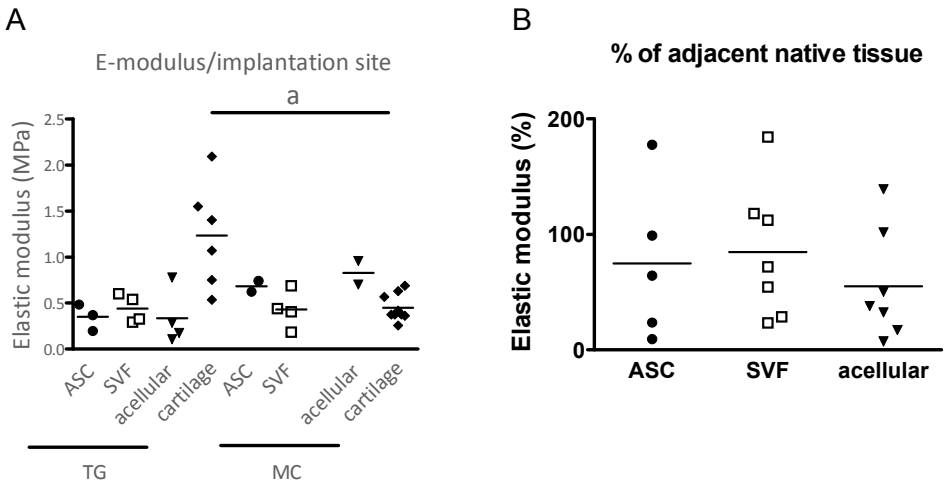

Figure 6. *Mechanical properties of constructs after indentation testing. (A) Elastic modulus of the constructs per implantation site. A large spreading in elastic modulus between the different samples can be observed. (B) Elastic modulus corrected to native tissue. the SVF-treated group again resembled the native tissue best, followed by the ASC-treated group and the acellular group being last. Both in the SVF-treated group as the ASC treated group 1 sample is missing due to technical flaws; moreover 3 samples are missing in the ASC-treated group due to inflammation.*

this variation due to implantation site and each individual goat, treatment over native tissue scores were also compared between the three different groups. Due to large variation, no significance was reached between all groups (p=0.27, Fig 6b). The SVF-treated group contained the largest number of samples approaching native values.

DISCUSSION

In this pilot study, applying a one-step surgical treatment of focal osteochondral defects in the caprine knee, we compared the regenerative potential of collagen type I/III scaffolds seeded with freshly isolated adipose derived stromal cells (SVF) with those seeded with cultured adipose stem cells (ASCs) or vehicle (acellular scaffolds). Tissue repair was rapid and after 4 weeks some regeneration could already be observed (ASCs > SVF > acellular), as visualized by immunohistological analyses. After 4 months the regenerative process had clearly progressed, based on immunohistological, biochemical, microCT, and biomechanical parameters. Remarkably, the SVF-treated group now tended to show better regeneration than the ASC-treated group, indicating a catch-up phenomenon by the SVF-group relative to the ASC-treated group. The better result for the ASC-group compared to the SVF-group at the 4-week time-point may be due to lower initial stem cell numbers implanted in the SVF-group (in retrospect ranging from 1.0-3.35*10^5 ASCs based on CFU-F assays) compared to the standardized 5*10^5 cultured ASCs in the ASC-group. The SVF catch-up phenomenon

observed after 4 months may be contributed to other cell types residing in the SVF like lymphocytes, pericytes and vascular smooth muscle cells, possibly leading to synergistic effects on the regenerative process at later stages. Together, these data suggest that for optimal cartilage regeneration, application of SVF may be favored over cultured ASCs.

As indicated above, we implanted collagenous scaffolds seeded with $5.0*10^5$ ASC or $5.0*10^6$ SVF cells (the latter based on our previous studies expected to contain approximately $1\text{-}5*10^5$ ASC-like cells[12]. This collagen I/III scaffold, containing oriented pores, was tested before in rabbits[33] and has already shown promising short- and mid-term results in the clinical setting in combination with chondrocytes to regenerate chondral defects[34]. Since we seeded our stem cell preparations according to the 'dropping on' method (http://www.optimaix.com/OptiMaix_Flyer_web.pdf) to the upper side of the scaffold, we assume that most of the applied cells would remain in the upper (chondral) part of our scaffold. As the total volume of the chondral part of the defect was about 20 mm^3, this would imply a cell density of $2.5*10^4$ cells/mm^3. This would match well with data on the structural organization of cartilage tissue, describing a cellular density of 24,000 cells per mm^3 at the articular surface decreasing three-and-a-half fold to about 7000 cells per mm^3 at the lower half of the upper radial zone[35] and with studies emphasizing high density to favour chondrogenesis[36,37]. Currently it is unclear whether application of even higher cell densities would give better results and this might certainly be interesting to investigate in future experiments.

The acellular control in fact mimicked the well known (modified) subchondral drilling or microfracture technique, allowing influx of cells from the underlying bone marrow compartment into the scaffold material. This method is widely used, although there is still controversy about its efficacy, and the quality and functionality of the tissue formed[238,39]. Nowadays, many studies aim at accelerated cartilage repair by augmenting the scaffolds with either autologous articular chondrocytes cultured from biopsies of non-weightbearing local cartilage, or mesenchymal stem cells like we did in this study. As stated above, the addition of freshly isolated SVF or cultured ASC into the collagen scaffold contributed to better regeneration of the cartilage and subchondral bone. However, how these cells exert this regeneration effect is yet unsolved, and is currently a hot topic in the regenerative medicine field: the cells may themselves differentiate into the desired phenotype, they may recruit and activate local mesenchymal stem cells towards regeneration, or they may reactivate local differentiated cells for this purpose. In orther words: the early regenerative effect in both cell-treated groups may be due to the paracrine or trophic effect of the stem cells on residing cells rather than their innate differentiation potential. This paracrine effect of stem cells has also been suggested by others to be more important than the differentiation potential of the cells[40-44]. This is prompted by studies that either found that only 8-33% of the defect's cell population arose from the implant itself[45,46] or, in the case of implanting chondrocytes, had no additional contribution at all[47,48]. Although the study setup does not allow conclusive statements about the actual mechanism of action of the seeded adipose stromal/stem cells, this study consistently showed a positive influence of the implanted cells on the overall regeneration process.

Retainment of a scaffold material in the defect site has been a major challenge in cartilage repair. If scaffold materials are too stiff, they easily get detached from the

surrounding cartilage[49,50]. Several scaffold anchoring strategies have been employed, such as suturing to the adjacent 'healthy' cartilage, and the use of hydrogels or sealant to glue the scaffold material to the defect site. However, suturing trauma may lead to osteoarthitic degeneration of the adjacent cartilage[51], and human fibrin sealant (Tissucol®) may cause immune reactions leading to cell death[52]. Tissue reactions to Tissucol were also observed in our pre-pilot study (suppl. 1), but we cannot currently rule out that this could be a result of its cross-species use. Eventually, we avoided scaffold loss by a combination of an osteochondral defect allowing press-fitting of the implanted scaffold, suturing onto adjacent cartilage, and postoperative immobilization. The latter, achieved by using a special designed Softcast® to immobilize the goat knees for 4 weeks, reduced shear to a large extent thus preventing scaffold loss effectively. Actually, by the slight muscle atrophy occurring in this 4-week period, movement and loading of the knee within the cast increased gradually, which probably facilitated and enhanced scaffold integration and cartilaginous differentiation. Whether this immobilization phase should be added in the clinical phase as well remains to be determined.

Not only the addition of regeneration-competent cells, but also the implantation site may influence the extent of regeneration, as illustrated by the differences in elastic moduli of the medial condyle and trochlear groove native tissues. Probably the biomechanical load might be of critical importance in this regard, i.e. the higher the biomechanical stress, the stronger the bone and the thicker the overlying cartilage[53,54]. As a consequence, the elastic modulus depends on anatomical location and on cartilage thickness as was shown by Athanasiou already in 1994[55]. If biomechanical stimuli are prime contributors to the extent of regeneration, this could be an explanation for the wide range of regeneration found between various studies, and this would be an argument for describing results as percentage of the native tissue to exclude this covariate, as was frequently done in this study. Although this might overcome confounding data and indentation testing is widely used to analyze the mechanical characteristics, it might be less reliable in thin cartilage, as Fischer warned for in his paper on limitations of indentation measurements[56]. Taking this into account, (too deep) indentation measurements and concomitant values of the underlying subchondral bone might have resulted in confounding data. These results thus have to interpreted with care.

Taken together, this study shows the potency of freshly isolated adipose stromal cells in a one-step surgical procedure to regenerate osteochondral defects. In addition to aforementioned arguments of patient friendliness and cost effectiveness by avoiding a second surgical intervention, the availability of commercial systems for intra-operative processing of adipose tissue, meeting GMP conditions and lowering the risk of infection instigated by "open" processing and prolonged culturing, are important advantages over the current concepts of tissue engineering strategies using cultured cells.

REFERENCES

1. Hunziker EB, 2002. Articular cartilage repair: basic science and clinical progress. A review of the current status and prospects, *Osteoarthritis.Cartilage.*, **10**: 432-463
2. Bouwmeester PS, Kuijer R, Homminga GN, Bulstra SK, and Geesink RG, 2002. A retrospective analysis of two independent prospective cartilage repair studies: autogenous perichondrial grafting versus subchondral drilling 10 years post-surgery, *J.Orthop.Res.*, **20**: 267-273
3. Brittberg M, 2009. Cell Carriers as the Next Generation of Cell Therapy for Cartilage Repair: A Review of the Matrix-Induced Autologous Chondrocyte Implantation Procedure, *Am.J.Sports Med.*, **38**: 1259-1271
4. Peterson L, Minas T, Brittberg M, Nilsson A, Sjogren-Jansson E, and Lindahl A, 2000. Two- to 9-year outcome after autologous chondrocyte transplantation of the knee, *Clin.Orthop.Relat Res.*, 212-234
5. Zuk PA, Zhu M, Mizuno H, Huang J, Futrell JW, Katz AJ, Benhaim P, Lorenz HP, and Hedrick MH, 2001. Multilineage cells from human adipose tissue: implications for cell-based therapies, *Tissue Eng*, **7**: 211-228
6. Li WJ, Chiang H, Kuo TF, Lee HS, Jiang CC, and Tuan RS, 2009. Evaluation of articular cartilage repair using biodegradable nanofibrous scaffolds in a swine model: a pilot study, *J.Tissue Eng Regen.Med.*, **3**: 1-10
7. Schoen I, Rahne T, Markwart A, Neumann K, Berghaus A, and Roepke E, 2009. Cartilage replacement by use of hybrid systems of autologous cells and polyethylene: an experimental study, *J.Mater.Sci.Mater. Med.*, **20**: 2145-2154
8. Chung C and Burdick JA, 2009. Influence of three-dimensional hyaluronic acid microenvironments on mesenchymal stem cell chondrogenesis, *Tissue Eng Part A*, **15**: 243-254
9. Steinert AF, Palmer GD, Pilapil C, Noth U, Evans CH, and Ghivizzani SC, 2009. Enhanced in vitro chondrogenesis of primary mesenchymal stem cells by combined gene transfer, *Tissue Eng Part A*, **15**: 1127-1139
10. Hwang NS, Varghese S, and Elisseeff J, 2008. Derivation of chondrogenically-committed cells from human embryonic cells for cartilage tissue regeneration, *PLoS. One.*, **3**: e2498-
11. Helder MN, Knippenberg M, Klein-Nulend J, and Wuisman PI, 2007. Stem Cells from Adipose Tissue Allow Challenging New Concepts for Regenerative Medicine, *Tissue Eng*, **13**: 1799-1808
12. Jurgens WJ, van DA, Doulabi BZ, Niessen FB, Ritt MJ, van Milligen FJ, and Helder MN, 2009. Freshly isolated stromal cells from the infrapatellar fat pad are suitable for a one-step surgical procedure to regenerate cartilage tissue, *Cytotherapy.*, **11**: 1052-1064
13. Jurgens WJ, Kroeze RJ, Bank RA, Ritt MJ, and Helder MN, 2011. Rapid attachment of adipose stromal cells on resorbable polymeric scaffolds facilitates the one-step surgical procedure for cartilage and bone tissue engineering purposes, *J.Orthop.Res.*, **29**: 853-860
14. Lu ZF, Zandieh DB, Wuisman PI, Bank RA, and Helder MN, 2007. Differentiation of adipose stem cells by nucleus pulposus cells: configuration effect, *Biochem.Biophys.Res. Commun.*, **359**: 991-996
15. Jurgens WJ, Oedayrajsingh-Varma MJ, Helder MN, Zandiehdoulabi B, Schouten TE, Kuik DJ, Ritt MJ, and van Milligen FJ, 2008. Effect of tissue-harvesting site on yield of stem cells derived from adipose tissue: implications for cell-based therapies, *Cell Tissue Res.*, **332**: 415-426
16. Ahern BJ, Parvizi J, Boston R, and Schaer TP, 2009. Preclinical animal models in single site cartilage defect testing: a systematic review, *Osteoarthritis.Cartilage.*, **17**: 705-713
17. Jackson DW, Lalor PA, Aberman HM, and Simon TM, 2001. Spontaneous repair of full-thickness defects of articular cartilage in a goat model. A preliminary study, *J.Bone Joint Surg.Am.*, **83-A**: 53-64
18. Driesang IM and Hunziker EB, 2000. Delamination rates of tissue flaps used in articular cartilage repair, *J.Orthop.Res.*, **18**: 909-911
19. Moran ME, Kim HK, and Salter RB, 1992. Biological resurfacing of full-thickness defects in patellar articular cartilage of the rabbit. Investigation of autogenous periosteal grafts subjected to continuous passive motion, *J.Bone Joint Surg.Br.*, **74**: 659-667
20. Niederauer GG, Niederauer GM, Cullen LC, Jr., Athanasiou KA, Thomas JB, and Niederauer MQ, 2004. Correlation of cartilage stiffness to thickness and level of

degeneration using a handheld indentation probe, *Ann.Biomed.Eng*, **32**: 352-359

21. Young AA, Appleyard RC, Smith MM, Melrose J, and Little CB, 2007. Dynamic biomechanics correlate with histopathology in human tibial cartilage: a preliminary study, *Clin.Orthop.Relat Res.*, **462**: 212-220
22. Cousins WJ, Armstrong RW, and Robinson WH, 1975. Young's modulus of lignin form a continuous indentation test, *J.Mater.Sci.*, **10**: 1655-1658
23. Athanasiou KA, Rosenwasser MP, Buckwalter JA, Malinin TI, and Mow VC, 1991. Interspecies comparisons of in situ intrinsic mechanical properties of distal femoral cartilage, *J.Orthop.Res.*, **9**: 330-340
24. O'Driscoll SW, Marx RG, Beaton DE, Miura Y, Gallay SH, and Fitzsimmons JS, 2001. Validation of a simple histological-histochemical cartilage scoring system, *Tissue Eng*, **7**: 313-320
25. Takahashi S, Oka M, Kotoura Y, and Yamamuro T, 1995. Autogenous callo-osseous grafts for the repair of osteochondral defects, *J.Bone Joint Surg. Br.*, **77**: 194-204
26. Noguchi T, Oka M, Fujino M, Neo M, and Yamamuro T, 1994. Repair of osteochondral defects with grafts of cultured chondrocytes. Comparison of allografts and isografts, *Clin. Orthop.Relat Res.*, 251-258. **302:** 251-258
27. Wakitani S, Goto T, Pineda SJ, Young RG, Mansour JM, Caplan AI, and Goldberg VM, 1994. Mesenchymal cell-based repair of large, full-thickness defects of articular cartilage, *J.Bone Joint Surg.Am.*, **76**: 579-592
28. Moojen DJ, Saris DB, uw Yang KG, Dhert WJ, and Verbout AJ, 2002. The correlation and reproducibility of histological scoring systems in cartilage repair, *Tissue Eng*, **8**: 627-634
29. Renders GA, Mulder L, Langenbach GE, and Koolstra JH, 2009. Contrast-enhanced microCT for assessment of articular cartilage and bone morphology in the jaw joint, *Bone*, **44**: s253-s338
30. Xie L, Lin AS, Guldberg RE, and Levenston ME, 2010. Nondestructive assessment of sGAG content and distribution in normal and degraded rat articular cartilage via EPIC-microCT, *Osteoarthritis.Cartilage.*, **18**: 65-72
31. Palmer AW, Guldberg RE, and Levenston ME, 2006. Analysis of cartilage matrix fixed charge density and three-dimensional morphology via contrast-enhanced microcomputed tomography, *Proc.Natl. Acad.Sci.U.S.A*, **103**: 19255-19260
32. Nuzzo S, Lafage-Proust MH, Martin-Badosa E, Boivin G, Thomas T, Alexandre C, and Peyrin F, 2002. Synchrotron radiation microtomography allows the analysis of three-dimensional microarchitecture and degree of mineralization of human iliac crest biopsy specimens: effects of etidronate treatment, *J.Bone Miner.Res.*, **17**: 1372-1382
33. Willers C, Chen J, Wood D, Xu J, and Zheng MH, 2005. Autologous chondrocyte implantation with collagen bioscaffold for the treatment of osteochondral defects in rabbits, *Tissue Eng*, **11**: 1065-1076
34. Manfredini M, Zerbinati F, Gildone A, and Faccini R, 2007. Autologous chondrocyte implantation: a comparison between an open periosteal-covered and an arthroscopic matrix-guided technique, *Acta Orthop.Belg.*, **73**: 207-218
35. Hunziker EB, Quinn TM, and Hauselmann HJ, 2002. Quantitative structural organization of normal adult human articular cartilage, *Osteoarthritis.Cartilage.*, **10**: 564-572
36. Concaro S, Nicklasson E, Ellowsson L, Lindahl A, Brittberg M, and Gatenholm P, 2008. Effect of cell seeding concentration on the quality of tissue engineered constructs loaded with adult human articular chondrocytes, *J.Tissue Eng Regen. Med.*, **2**: 14-21
37. Troken A, Marion N, Hollister S, and Mao J, 2007. Tissue engineering of the synovial joint: the role of cell density, *Proc.Inst.Mech. Eng H.*, **221**: 429-440
38. Khan WS, Johnson DS, and Hardingham TE, 2010. The potential of stem cells in the treatment of knee cartilage defects, *Knee.*, **17**: 369-374
39. Menche DS, Frenkel SR, Blair B, Watnik NF, Toolan BC, Yaghoubian RS, and Pitman MI, 1996. A comparison of abrasion burr arthroplasty and subchondral drilling in the treatment of full-thickness cartilage lesions in the rabbit, *Arthroscopy*, **12**: 280-286
40. Chamberlain G, Fox J, Ashton B, and Middleton J, 2007. Concise review: mesenchymal stem cells: their phenotype, differentiation capacity, immunological features, and potential for homing, *Stem Cells*, **25**: 2739-2749
41. Charriere G, Cousin B, Arnaud E, Andre M, Bacou F, Penicaud L, and Casteilla L, 2003. Preadipocyte conversion to macrophage.

Evidence of plasticity, *J.Biol.Chem.*, **278**: 9850-9855

42. Jansen BJ, Gilissen C, Roelofs H, Schaap-Oziemlak A, Veltman J, Raymakers RA, Jansen J, Kogler G, Figdor CG, Torensma R, and Adema GJ, 2009. Functional differences between mesenchymal stem cell populations are reflected by their transcriptome. Stem Cells Dev **9**: 481-490.
43. Mitchell JB, McIntosh K, Zvonic S, Garrett S, Floyd ZE, Kloster A, Di Halvorsen Y, Storms RW, Goh B, Kilroy G, Wu X, and Gimble JM, 2006. Immunophenotype of human adipose-derived cells: temporal changes in stromal-associated and stem cell-associated markers, *Stem Cells*, **24**: 376-385
44. Wu L, Leijten JC, Georgi N, Post JN, Van Blitterswijk CA, and Karperien M, 2011. Trophic Effects of Mesenchymal Stem Cells Increase Chondrocyte Proliferation and Matrix Formation, *Tissue Eng Part A*,
45. Grande DA, Pitman MI, Peterson L, Menche D, and Klein M, 1989. The repair of experimentally produced defects in rabbit articular cartilage by autologous chondrocyte transplantation, *J.Orthop. Res.*, **7**: 208-218
46. Zarnett R and Salter RB, 1989. Periosteal neochondrogenesis for biologically resurfacing joints: its cellular origin, *Can.J.Surg.*, **32**: 171-174
47. Breinan HA, Minas T, Hsu HP, Nehrer S, Sledge CB, and Spector M, 1997. Effect of cultured autologous chondrocytes on repair of chondral defects in a canine model, *J.Bone Joint Surg.Am.*, **79**: 1439-1451
48. Mierisch CM, Wilson HA, Turner MA, Milbrandt TA, Berthoux L, Hammarskjold ML, Rekosh D, Balian G, and Diduch DR, 2003. Chondrocyte transplantation into articular cartilage defects with use of calcium alginate: the fate of the cells, *J.Bone Joint Surg.Am.*, **85-A**: 1757-1767
49. Drobnic M, Radosavljevic D, Ravnik D, Pavlovcic V, and Hribernik M, 2006. Comparison of four techniques for the fixation of a collagen scaffold in the human cadaveric knee, *Osteoarthritis.Cartilage.*, **14**: 337-344
50. Brehm W, Aklin B, Yamashita T, Rieser F, Trub T, Jakob RP, and Mainil-Varlet P, 2006. Repair of superficial osteochondral defects with an autologous scaffold-free cartilage construct in a caprine model: implantation method and short-term results, *Osteoarthritis. Cartilage.*, **14**: 1214-1226
51. Hunziker EB and Stahli A, 2008. Surgical suturing of articular cartilage induces osteoarthritis-like changes, *Osteoarthritis. Cartilage.*, **16**: 1067-1073
52. van Susante JL, Buma P, Schuman L, Homminga GN, van den Berg WB, and Veth RP, 1999. Resurfacing potential of heterologous chondrocytes suspended in fibrin glue in large full-thickness defects of femoral articular cartilage: an experimental study in the goat, *Biomaterials*, **20**: 1167-1175
53. Andriacchi TP, Koo S, and Scanlan SF, 2009. Gait mechanics influence healthy cartilage morphology and osteoarthritis of the knee, *J.Bone Joint Surg.Am.*, **91 Suppl 1**: 95-101
54. Koo S, Gold GE, and Andriacchi TP, 2005. Considerations in measuring cartilage thickness using MRI: factors influencing reproducibility and accuracy, *Osteoarthritis. Cartilage.*, **13**: 782-789
55. Athanasiou KA, Agarwal A, and Dzida FJ, 1994. Comparative study of the intrinsic mechanical properties of the human acetabular and femoral head cartilage, *J.Orthop.Res.*, **12**: 340-349
56. Fischer-Cripps AC, 2011. Critical review of analysis and interpretation of nanoindentation test data, *Surface & Coatings Technology*, **200**: 4153-4165

SUPPLEMENTS

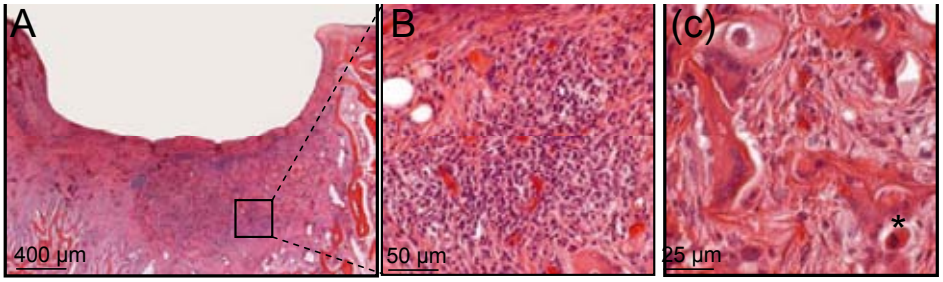

Supplementary figure 1. *Inflammatory (immune) respons due to fibrin sealant. (A) overview of the implanted scaffold, filled with inflammatory cells. (B) Magnification of A, in which polymorphonuclear cells can be observed. (C) giant body cell, indicative of massive immune respons (marked by asterisk).*

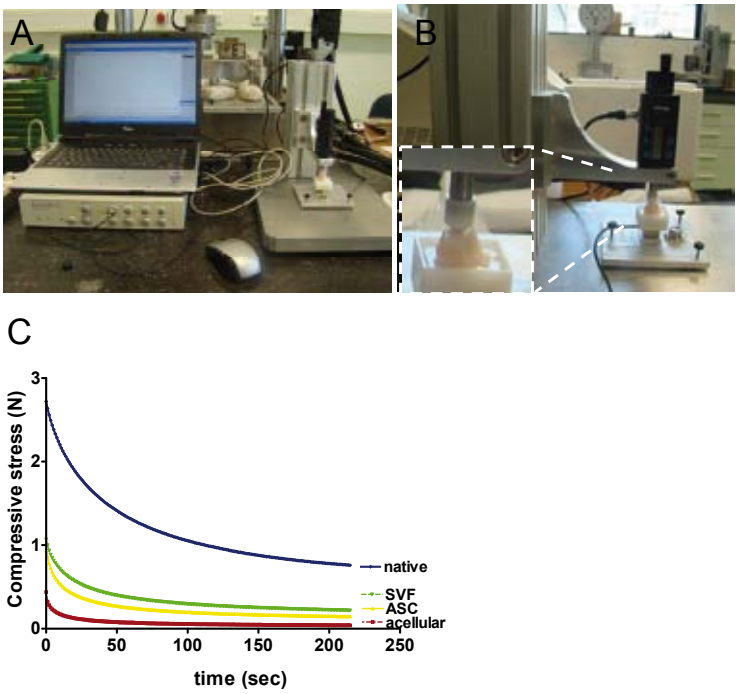

Supplementary figure 2. *Set-up of mechanical test. (A) benchtop indenter to the right, with on the left laptop for data analyzing. (B) Close-up of indenter, with display showing indentation height, and stage on which each specimen was placed. (C) Representative example of mechanical response to indentation (200 µm) showing stress-relaxation curve of the three constructs and native tissue of the trochlear groove. Native tissue showed highest stress peaks, followed by the SVF- and ASC-treated group; the acellular groups showed the lowest stress peak.*

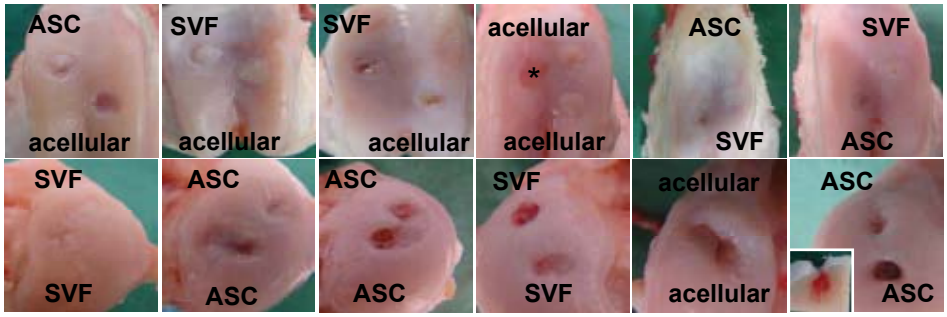

Supplementary figure 3. *Gross appearance of all experimental implants (A) Implants of all groups showed variable regeneration. Trochlear implants tended to show better regeneration than implants on the medial condyle. The inlay within the last picture shows a longitudinal transsection through an implant suffering from chronic inflammation. No regeneration of the cartilage was observed, but abundant infiltration of blood and inflammatory cells into the subchondral bone. Asterisk marks cartilage defect which was left empty due to faulty burring.*

Supplement 4 *Table histology. Microscopic Appearance of All Defects, Based on the Histologic Scoring System. A Perfect Score For All Items Is 21 Points.*

Category	Implantation Site	Implantation Time (Months)	Surface Irregularity	Bonding to Adjacent Cartilage	Regenerated Subchondral Bone
Control1	TG	1	0.5	1	0
Control2	TG	1	1	1.5	0.5
Control3	TG	4	0	2	1
Control4	TG	4	2	2	1
Control5	TG	4	1	2	1
Control6	TG	4	3	1.5	0.5
Control7	TG	4	2.5	2	1
Control8	MC	4	3	2	1
Control9	MC	4	3	2	1
SVF1	MC	1	0	1	0
SVF2	MC	1	0	2	0
SVF3	TG	1	1	2	0
SVF4	MC	4	0.5	2	1.5
SVF5	MC	4	3	2	2
SVF4	TG	4	3	2	2
SVF5	TG	4	2.5	2	0.5
SVF6	MC	4	2	2	2
SVF7	MC	4	2	2	1
SVF8	TG	4	3	2	1
SVF9	TG	4	2.5	2	1
ASC1	TG	1	0	1	0
ASC2	MC	1	1.75	2	0
ASC3	MC	1	1.5	1.5	0
ASC4	TG	4	2	2	0
ASC5	MC	4	0	2	0
ASC6	MC	4	3	2	1
ASC7	MC	4	1.5	2	0.5
ASC8	MC	4	1.5	2	1
ASC9	TG	4	3	2	0
ASC10	MC	4	1.5	2	2
ASC11	MC	4	2	2	1
ASC12	TG	4	2	2	2
Max score			3	2	2

MC=medial condyle. TG=trochlear groove

Inflammatory Cell Infiltration around Implant	Chondrocyte Clustering	Freedom from Degenerative changes in adjacent cartilage	Metachromasia	Hyalinity	Total
2	0	2.5	0	0	6
1.5	0	1.5	0	0.5	6.5
2	0	2	1	1	9
2	0	2	2	2	13
1.5	0	2	1	1	9.5
2	1	2	2	2	14
2	1.5	2	2	2	15
2	2	2.5	2.5	2	17
2	1.5	2	3	2	16.5
1.5	0.5	2	0.5	0.5	6
1.5	0	1.5	0	0	5
2	0	1.5	0.5	0.5	7.5
2	1.5	2	3	2	14.5
2	1.5	2.5	3	2.5	18.5
2	2	2	3	2.5	18.5
1	0	2	1	1	10
2	1.5	1	2	2.5	15
2	1	2.5	1.5	2	14
2	1.5	2	1	2	14.5
2	1.5	2	2	2	15
2	0	2	0	0	5
2	1	2.75	2.25	2.5	14.25
1.5	0.5	2	0.75	1	10.75
2	0	1	1	1	9
2	0	2	1.5	1	8.5
2	1	2	3	2.5	16.5
1	0	2	0.5	1	8.5
1	0	2	1	1	9.5
1	1.5	2	2	2	13.5
2	1.5	3	1.5	1.5	15
1	1	2	1.5	2	12.5
2	1	2	1	2	14
2	2	3	3	4	21

Supplemental data *5. Table MicroCT. Data on bone and cartilage regeneration of implanted constructs.*

	Native MC	Native TG	Acellular	SVF	ASC
	(n=12)	(n=12)	(n=7)	(n=8)	(n=9)
Chondrogenesis	raw	raw	% of native [#]	% of native [#]	% of native [#]
Attenuation	1.23 ± 0.31	1.45 ± 0.39	113.0± 28.6	95.3 ± 22.9	104.0 ± 26.4
Osteogenesis	raw	raw	% of native	% of native	% of native
BV/TV (%)	59.3 ± 11.9	52.7 ± 15.5	62.9 ± 21.1	65.2 ± 28.3	63.2 ± 22.4
DMB (mg HA/cm^3)	767.4 ± 54.2	778.1 ± 29.3	91.2 ± 6.4	91.1 ± 3.0	92.2 ± 4.4

All data are depicted as mean ± SD. MC = medial condyle, TG = trochlear groove.
[#] % of native data of each sample of all groups are corrected to adjoining implantation site.